

Row Following in Pergola Structured Orchards*

Jamie Bell, Bruce A. MacDonald, and Ho Seok Ahn

Abstract— Mobile service robots have the potential to improve the efficiency of fruit production in orchards. One of the key tasks that such robots must perform is traversing the rows. Many of the past implementations of row following in orchards have been developed for rows where the trees appear like walls on both sides. Another orchard structure that is used is the pergola, where a sparse array of trunks and posts hold up a canopy, which resembles a ceiling. Navigation in pergola structured environments has received less attention. The variations in the pergola environment- including the presence of tall weeds, hanging branches, undulating terrain and varying geometry- make following the rows a challenging problem. This paper presents solutions for finding the row centreline in pergola structured environments, in the presence of real world variability. A 3D laser scanner is used to measure the positions of posts and trunks, amongst the other features in the pergola. From the extracted features, the mode gradient of nearest neighbours is used to find the row direction and hence the centreline. The practicality of the system is demonstrated by autonomously driving a mobile robot through over 5000 meters of a kiwifruit orchard with a pergola structure, using the row detection method. This method performs favourably compared to an existing method of row detection in kiwifruit orchards.

I. INTRODUCTION

This paper is a part of a wider study of the application of mobile robotics to improve the productivity of fruit production by performing repetitive and labor intensive tasks in orchards. In particular, this paper focuses on row detection and following in GPS denied structured orchard environments.

Orchards are designed with a variety of structures. It is common for orchard rows to consist of dense tree walls on both sides of a row (Fig. 1). The pergola is another structure used, where trunks and posts support an overhead canopy of beams, branches and leaves (Fig. 2). Fruits such as grapes, kiwifruit, passionfruit and nashi pears may be grown with a pergola structure [1-3].

The problem that is addressed in this paper is the measurement of the linear and angular offset from a row centreline in real-world pergola structured environments (Fig. 3). The sensor used is a multi-plane laser scanner (Velodyne VLP-16). The approach taken in this paper is to use the posts and trunks as features, representing the sides of a row. The detection of these features is complicated by the variability in pergola structures including, differing dimensions, uneven terrain, tall weeds and hanging branches.

*Research supported by the New Zealand Ministry for Business, Innovation and Employment (MBIE) on contract UOAX1414.

The authors are with the Department of Electrical and Computer Engineering, University of Auckland, New Zealand.

J. Bell (correspondence: jbel060@aucklanduni.ac.nz, +64 21 276 1114).

B. A. MacDonald (b.macdonald@auckland.ac.nz).

H. S. Ahn (hs.ahn@auckland.ac.nz).



Figure 1. An apple orchard with tree walls on both sides of the row.



Figure 2. Sparse posts and trunks below the canopy in a kiwifruit orchard with a pergola structure. Note the weeds, hanging branches, undulating terrain and possible row direction ambiguity transverse to the true row direction, caused by the sparseness and regular pattern of the pergola.

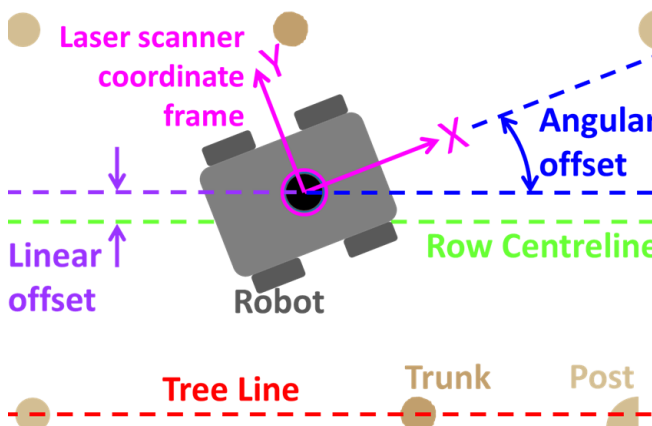


Figure 3. A diagram of a horizontal cross-section of a row. Trunks and posts form tree-lines on both sides of the row. A robot is shown in grey with its main direction of travel aligned with the x-axis of the laser scanner. Row detection is defined as the task of finding the linear and angular offset of the laser scanner from the row centreline. Note that the terms and coordinate system in this diagram are used throughout this paper.

The measurements of the linear and angular offset, which are outputs from the row detection system, are used as feedback for a row driving control system on a specialty crop service robot prototype.

A. Literature Survey

There have been various autonomous mobile robots, developed for agricultural tasks, which use some combination of a GPS variant and other sensors [4, 5]. However, GPS is unreliable in many types of orchards [5, 6] and, in particular, under the canopy of a pergola structure.

In past analyses of the problem of orchard navigation, 2D laser scanners have been identified as an effective option that allows for localization, mapping and obstacle avoidance [7]. 2D laser scanners were favored over 3D laser scanners because of cost differences, although with the recent emergence of more affordable 3D sensors, such as those from Velodyne and Quanergy, this position could be reassessed.

There have been various examples of mobile robots navigating through orchards, where tree walls line the rows. Subramanian et al. used a camera and 2D laser scanner mounted on the cab of a tractor and angled down towards the ground [8]. Lines were fitted to the tree walls in the camera images and discontinuities in the laser scans were detected as trees. However, computer vision has been argued to be difficult in kiwifruit orchards because of the highly variable lighting conditions and possible occlusion of the tree-line by weeds and hanging branches [9]. The approach of using an angled down laser scanner would be less useful in a pergola structured orchard because of the sparseness of features such as trunks and posts. If a 2D laser scanner was used in a pergola structured orchard, it would generally detect more posts and trunks if it was horizontal.

Horizontal 2D laser scanners have been used in orchards to detect the tree walls and fit lines to the data to determine the current row centreline [10, 11]. However, such line fitting techniques may not work so well in pergola structured orchards because of the structural differences. In pergola structures the features that define the row direction are relatively sparse and a laser scanner has visibility of a wide area outside of the current row. As a result, the amount of data that defines the current row is small compared to the data from other features, which can include trees and trunks in adjacent rows, hedgerows surrounding an orchard block, hanging branches and tall weeds. As can be seen in Fig. 4, this data from other features can form strong candidates for line fitting and hence may produce false detections.

Detecting the row centreline in pergola structured orchards has been attempted by using a digital compass with a map as a prior and refining the row estimate using data from a 2D horizontal laser scanner [9]. The open issues from this work included handling the case where the ground or canopy intersects the laser scanner plane in the region of interest (Fig. 5). When this happens, there is less data from the trees and posts and the data from the ground or canopy can skew the result (Fig. 6). It may be possible to address this issue using 3D laser scanner data, using the additional planes to detect additional trunk and post features.

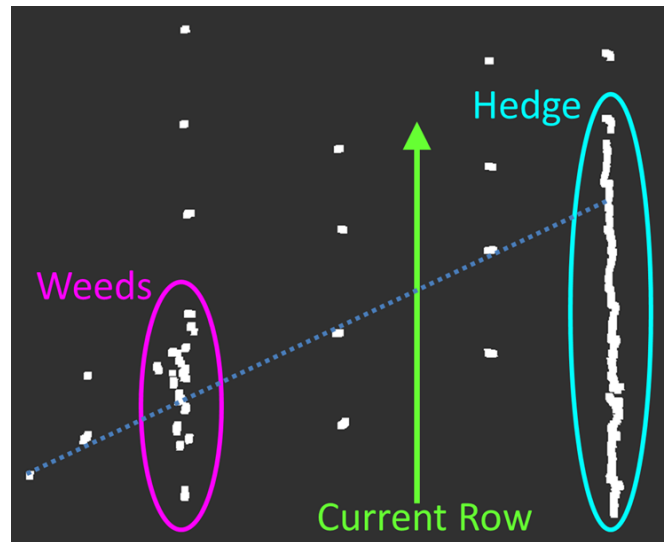


Figure 4. A horizontal 2D laser scan in a kiwifruit orchard, where there are strong candidates for line fitting from diagonals, nearby weeds and hedges.

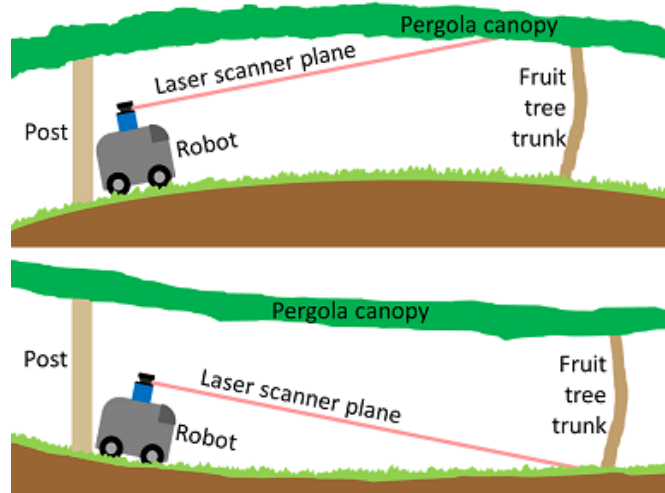


Figure 5. In a pergola structured environment, instead of detecting tree trunks and posts, a 2D laser scanner on a robot may detect the canopy on a convex slope (top) or the ground on a concave slope (bottom).

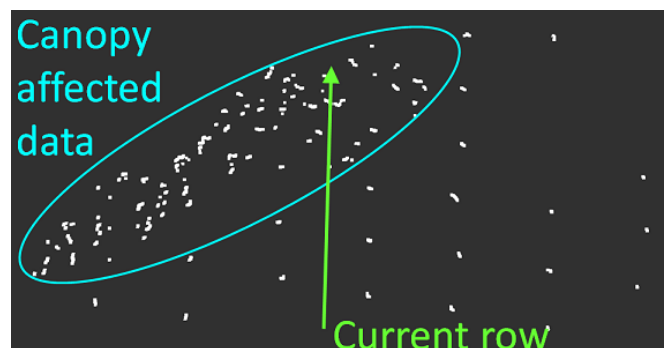


Figure 6. 2D laser scanner data where the canopy of the pergola is detected.

3D laser scanner data has been used before for navigation in orchards. Previously a 2D laser scanner on an oscillating platform was used to collect 3D point clouds of orchard rows in order to fit lines to the tree walls [12]; however, this method fitted to the strongest line candidate, which is not always a part of the current row (Fig. 4) or could be affected

by data from the ground or overhead canopy (Fig. 6) in an orchard with a pergola structure. In another implementation, a 2D laser scanner was used on a nodding platform to collect 3D data and detect the free space down a row, lined with tree walls [13]; however, in a pergola there is free space in multiple directions so there is the potential for false positive row detections with this method. In this paper a 3D sensor is used, as opposed to a rotated 2D laser scanner, and the application is autonomous driving in pergola structured environments, as opposed to rows lined with tree walls.

B. Outline

This paper describes methods for row centreline measurement and row following in pergola structured orchards. The key novel contributions of the methods described in this paper are:

- The use of laser scanner data from multiple adjacent rows to detect the current row heading.
- The method detects pergola rows without the need for additional sensors, such as a digital compass or prior maps.
- The use of a 3D laser scanner to allow data from post and trunk features to be collected at further ranges on undulating terrain.
- Methods to remove noise from the data caused by sloping terrain (as in Fig. 5), while filtering data from hanging branches, weeds and other objects in and close to the current row.
- The testing of the methods proposed here and a comparison with an existing algorithm in a real world pergola structured orchard environment.

The key methods used are described in section II. The test procedure, including the test robot setup, is described in section III. The results from testing are given in section IV. Conclusions and future work follow in sections V and VI respectively.

II. ROW CENTRELINE DETECTION & FOLLOWING

The major steps in the processing of the 3D laser scanner data for the row centreline detection and following were:

1. Feature extraction, where possible posts and trunks in the pergola were extracted from the laser scanner data.
2. Angular offset measurement, where the angle of the orchard rows with respect to the laser scanner's coordinate system was calculated.
3. Linear offset measurement, where the linear offset of the laser scanner from the row centreline was calculated.
4. Calculating steering commands from the angular and linear offset measurements.
5. Detecting and turning at the row ends to reinitialize row following.

These steps are described in more detail in the following sections.

A. Feature Extraction

The key insights that were used in the design of the post and trunk feature extractors from 3D laser scanner data in pergola structures were that:

- On a single plane, posts and trunks appear as smaller clusters of laser scan points than some other objects such as hedgerows, tractors or bins.
- On a single plane, which has measurements with a long range, posts and trunks generally appear separated from other clusters, whereas other objects such as weeds or the canopy may appear in clumps.
- Across multiple planes, the posts and trunks appear more consistently than shorter objects, such as weeds or hanging branches.

The steps for feature extraction began with clusters of laser scan points being found in each plane of the 3D laser scanner data using the method described by Scarfe [9]. Clusters with a length greater than a threshold were designated as unlikely to be posts or trunks; these clusters were removed from further consideration. In addition, any clusters within a set distance of a set number of other clusters were also removed. The results of these steps for a single plane of 3D laser scanner data are shown in Fig. 7.

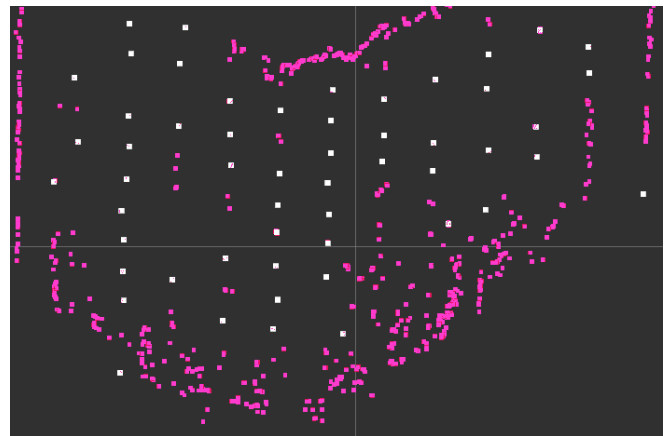


Figure 7. A single plane of 3D laser scanner data with the points used for further processing highlighted in white.

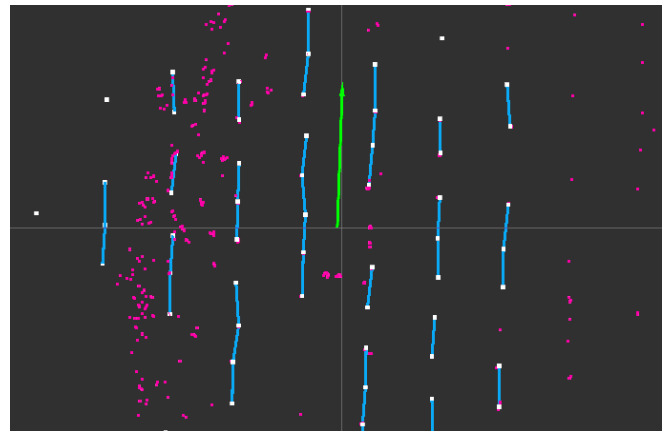


Figure 8. A single plane of 3D laser scanner data (magenta) with the points found by feature extraction highlighted in white, nearest neighbours indicated with blue and the detected row centreline (green arrow).

The clusters from multiple planes were grouped based on a threshold distance between clusters. The heights of the resulting groups were compared to a threshold to determine which were posts and trees. The resulting output from the feature extraction for a single 3D laser scan is shown as the white points in Fig. 8.

B. Row Centreline Angular Offset Measurement

The data output from the feature extraction was used for measurement of the angular offset from the row centreline. The key insights that were used in the angular offset measurement were that:

- Most posts and trunks are closer to other posts or trunks in the same tree-line than to an adjacent tree-line. This suggests that the angle between nearest neighbours should also be the angle of the tree-line and hence the angle of the orchard row centrelines.
- Multiple rows may be used to calculate the current row angular offset since rows are generally planted parallel to each other. This may increase the number of points used for angular offset calculation and hence increase the strength of the signal relative to the noise.

Using the data from feature extraction, each cluster's nearest neighbour was found. Nearest neighbours that were further apart than the row width were rejected to eliminate the possibility of using neighbours that were not in the same tree-line. The angles between the resulting nearest neighbours were calculated. The mode of the calculated angles was taken to be the current estimate of the angular offset from the row centreline.

C. Row Centreline Linear Offset Measurement

The angular offset measurement and an estimate of the row width were used to extract the data of the current row from the nearest neighbour pairs. Straight lines were fitted to the data on both sides of the row, corresponding to the left and right tree-lines. From the straight line formulae of the tree-lines, the linear distance offset measurement from the row centreline (d_c) was calculated by:

$$d_c = 0.5(c_l + c_r) \cos(\theta), \quad (1)$$

where c_l and c_r are the laser scanner coordinate system y intercepts of the left and right tree-line formulae,

θ is the row centreline angular offset measurement.

D. Row Following

Row following was implemented to test the practicality of the row detection system. The linear and angular offsets from the row centreline measurement were used to calculate steering angle commands according to:

$$k_1(d_c - d_y) + k_2(\theta - \alpha), \quad (2)$$

where d_y is the distance between the laser scanner's centre and the robot's centre in the y direction,

α is the angle between the laser scanner's x axis and the forward direction of the robot,

k_1 and k_2 are constants.

The constants were manually tuned so that when there was a significant linear offset the robot would steer towards the row centre but the robot would also straighten up as the linear offset reduced. The values d_y and α were found by hand measuring from a wall to points on the laser scanner mount and robot.

E. Row End Behavior

Row ends were detected by a lack of canopy above, which was achieved by checking for points in a fixed volume from the 3D laser scanner data. On detection of a row end, a fixed steering angle was commanded and continued to be commanded until the linear and angular offset from row detection were within set bounds, at which point the row following recommenced. The polarity of the row end turn was toggled in order to achieve the paths shown in Fig. 9.

III. TEST PROCEDURE

A. Test Setup

The 3D laser scanner used was a Velodyne VLP-16, which was setup to run at 10 Hz and mounted horizontally at a height of 0.8 of a metre from the ground. The software was run on a Dell E6410 laptop. The laser scanner and laptop were mounted on a temporary test platform, which was a Pioneer P3-AT mobile robot (Fig. 10).

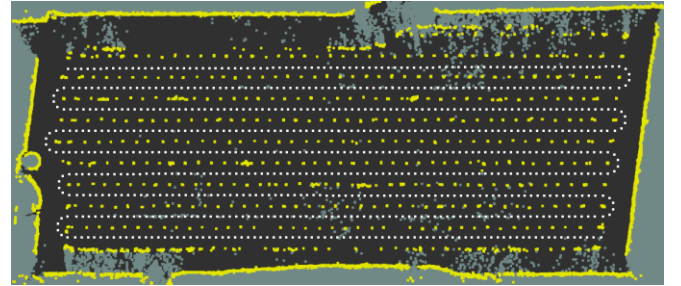


Figure 9. One of the paths traversed during autonomous driving in the kiwifruit orchard. Incidentally, this map was created using GMapping [14].



Figure 10. The Velodyne VLP-16 3D laser scanner, Pioneer P3-AT robot test platform and laptop used during autonomous driving.

B. Environment

The test setup was run in a gently sloping kiwifruit orchard block with gradients up to 15 percent. The weather was intermittently sunny and overcast. The orchard block consisted of 9 full rows of 110 meters length (Fig. 9). There were kiwifruit and pruned branches on the ground, weeds in the tree-lines, branches hanging down to 0.6 meters from the ground and some 0.1 meter deep holes.

C. Data Collection Parameters

The setup was run at 0.5 ms^{-1} ; faster speeds were not used because the setup was marginally stable when running over objects on the ground, while going downhill. The setup was run autonomously over 5000 meters, covering the orchard block used, with some rows traversed multiple times. The raw and processed laser scanner data was recorded for further analysis.

D. Hand Marked Up Data

A sample of the data collected was marked up by hand in order to provide a basis for comparison for row detection methods. The procedure followed for the marking up was to look at the 8th plane from bottom of the 3D laser scanner data. Points that seemed to be a part of the left tree-line of the row were selected and then the same was done for the right tree-line of the row. Lines were fitted to each tree-line. The average gradients and average y-axis intercepts of the tree-line formulae were calculated as the row centreline. The row centreline, defined in the 3D laser scanner's coordinate system, gave the linear and angular offset used for comparison in the results below.

IV. RESULTS

A. Autonomous Driving

The test platform completed over 5000 meters of autonomous row following throughout an orchard block without a single intervention for faults. As far as the authors know, this is a first in terms of real world driving testing for pergola structured orchards.

Row end turns were also attempted as a part of autonomous driving. The entire path shown in Fig. 9 was completed autonomously once without faults. However, in other attempts, the row end turns were not always completed due to the temporary test robot platform being physically unable to complete some turns when driving on an uphill slope.

B. Row Detection Comparison with Existing Method

The existing pergola structured row detection method of Scarfe [9] was coded, tuned and run using just the 8th plane from bottom of the 3D laser scanner data. The method described in section II was compared to Scarfe's method. For both methods the calculated linear and angular offset of the 3D laser scanner from the row centreline was compared to the linear and angular offset given by the hand marked up data. The results are shown in Fig. 11 and Fig. 12. The standard deviations of the same data are given in Table I.

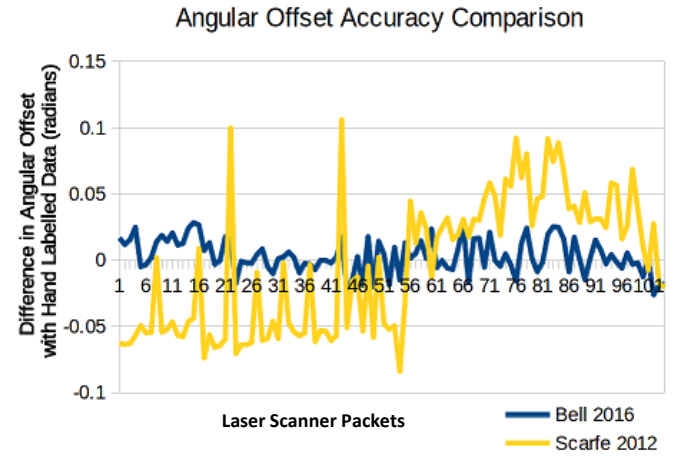


Figure 11. The difference between the angular offset calculated by each method and the angular offset given by the hand marked up data.

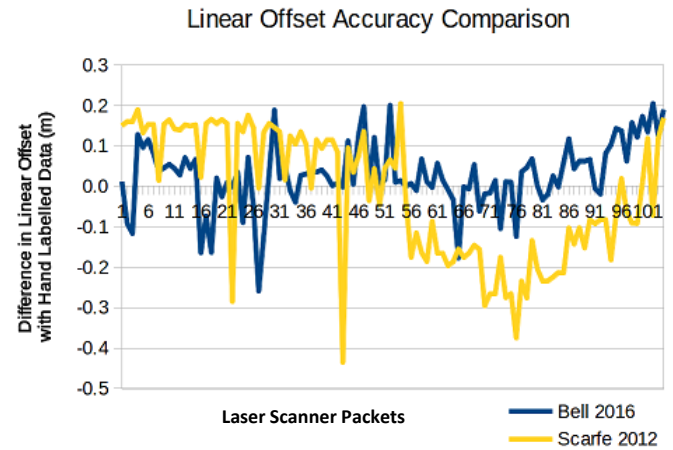


Figure 12. The difference between the linear offset calculated by each method and the linear offset given by the hand marked up data.

Table I. Standard deviations of the differences in centreline offsets between each method tested and the hand marked up data.

	Angular Offset Difference Standard Deviation (radians)	Linear Offset Difference Standard Deviation (m)
Bell 2016	0.01	0.08
Scarfe 2012	0.05	0.16

The method presented here seems to provide a significant increase in performance when considering angular offset measurement accuracy and a less significant improvement in the performance of linear offset accuracy. The reasons for the improvement in performance were analyzed by visually inspecting the drawn outputs; for example, Fig. 13. It seems that the method of Scarfe [9] can be prone to being affected by noise when there are many noise data points close to the current row. In contrast, the methods presented here have a stronger signal due to the consideration of multiple rows and multiple planes from the 3D laser scanner. In addition, the methods presented here also provide multiple stages to filter noise including the removal of oversized clusters, the removal of bunched clusters and taking the mode of nearest neighbours, during the angular offset calculation.

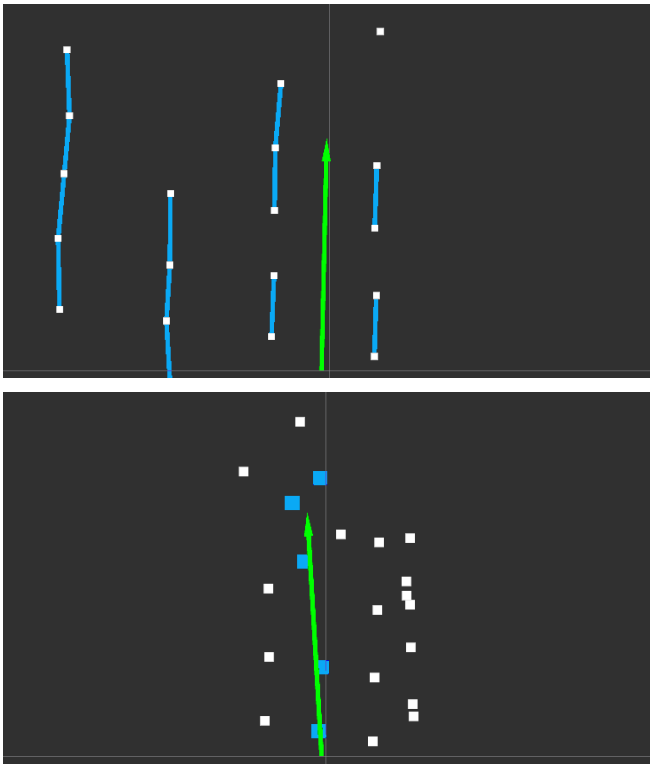


Figure 13. A comparison of the row centreline measurement (green arrow) at the same point in time from the method presented here (top) and Scarfe's method [9] (bottom). The points output from feature extraction are white. Blue represents the data used for the row centreline calculation. Scarfe's method appears to be less accurate when there are many noise data points after feature extraction.

V. CONCLUSIONS

The methods presented here represent early work in the development of algorithms for navigation in pergola structured orchards, using a 3D laser scanner. Compared to existing similar algorithms, the contributions of the methods presented here include methods to remove noise from the data, the use of multiple rows to determine the angular offset of the current row for the case of straight parallel rows and the use of a single 3D laser scanner for detecting the row centreline, as opposed to using multiple sensors and prior maps. In addition, the row following method, as well as the row end detection method and behaviour, are given here.

The row detection methods were successfully validated by performing autonomous driving throughout a kiwifruit orchard block with a pergola structure. The accuracy of row detection was compared to an existing algorithm, which was designed for pergola structured kiwifruit orchards, and was found to produce some improvement in performance, especially with regards to angular accuracy. Inspection of the test run data suggests that a key reason for this improvement is the ability of the methods presented here to deal with the real world pergola orchard environment's unstructured terrain, such as hanging branches, tall weeds or undulating terrain and canopy.

VI. FUTURE WORK

As can be seen in Fig. 9, work has started on creating maps from the laser scanner data. The result is that the robot

can traverse and map an orchard block. This will be further developed to create semantic maps with objects recognised from the laser scanner data. Ultimately, these components will be parts of a larger system that will be used to navigate large mobile robots through pergola structured orchards, performing useful functions, including spraying and harvesting.

VII. ACKNOWLEDGEMENTS

The authors would like to thank the entire orchard robotics team- including our partners from the University of Waikato, Robotics Plus and Plant & Food Research- for their help and support. The authors also very much appreciate the generosity of the Batemans for the use of their orchard during development and testing.

REFERENCES

- [1] D. I. Jackson, *Temperate and subtropical fruit production*. Wellington: Butterworths Horticultural Books, 1999.
- [2] R. E. Paull and O. Duarte, *Tropical Fruit* vol. 2. Oxfordshire: CABI Publishing, 2012.
- [3] K. Chalmers, *Hot Climate Wine Growing, Making and Marketing in Southern Italy and its Application in Australia*. Melbourne: International Specialised Skills Institute, 2013.
- [4] S. J. O. Corpe, T. Liqiong, and P. Abplanalp, "GPS-guided modular design mobile robot platform for agricultural applications," in *Sensing Technology (ICST), 2013 Seventh International Conference on*, 2013, pp. 806-810.
- [5] M. Li, K. Imou, K. Wakabayashi, and S. Yokoyama, "Review of research on agricultural vehicle autonomous guidance," *International Journal of Agricultural and Biological Engineering*, vol. 2, pp. 1-16, 2009.
- [6] Y. G. Ampatzidis, S. G. Vougioukas, D. D. Bochtis, and C. A. Tsatsarelis, "A yield mapping system for hand-harvested fruits based on RFID and GPS location technologies: field testing," *Precision Agriculture*, vol. 10, pp. 63-72, 2009.
- [7] H. Mousazadeh, "A technical review on navigation systems of agricultural autonomous off-road vehicles," *Journal of Terramechanics*, vol. 50, pp. 211-232, 2013.
- [8] V. Subramanian, T. F. Burks, and A. A. Arroyo, "Development of machine vision and laser radar based autonomous vehicle guidance systems for citrus grove navigation," *Computers and Electronics in Agriculture*, vol. 53, pp. 130-143, August 2006.
- [9] A. J. Scarfè, "Development of an Autonomous Kiwifruit Harvester: A thesis presented in partial fulfilment of the requirements for the degree of Doctor of Philosophy in Industrial Automation at Massey University, Manawatu, New Zealand," 2012.
- [10] O. C. Barawid Jr, A. Mizushima, K. Ishii, and N. Noguchi, "Development of an Autonomous Navigation System using a Two-dimensional Laser Scanner in an Orchard Application," *Biosystems Engineering*, vol. 96, pp. 139-149, October 2007.
- [11] S. Hansen, E. Bayramoglu, J. C. Andersen, O. Ravn, N. Andersen, and N. K. Poulsen, "Orchard navigation using derivative free Kalman filtering," in *American Control Conference (ACC)*, San Francisco, 2011, pp. 4679-4684.
- [12] J. Zhang, A. Chambers, S. Maeta, M. Bergerman, and S. Singh, "3D Perception for Accurate Row Following: Methodology and Results," presented at the 2013 IEEE/RSJ International Conference on Intelligent Robots and Systems (IROS), Tokyo, 2013.
- [13] S. J. Moorehead, C. K. Wellington, B. J. Gilmore, and C. Vallespi, "Automating orchards: a system of autonomous tractors for orchard maintenance," presented at the IEEE/RSJ International Conference on Intelligent Robots and Systems, Workshop on Agricultural Robotics, Algarve, Portugal, 2012.
- [14] G. Grisetti, C. Stachniss, and W. Burgard, "Improved Techniques for Grid Mapping with Rao-Blackwellized Particle Filters," *IEEE Transactions on Robotics*, vol. 23, pp. 34-46, 2007.